Fracture Mechanics of Concrete Structures
Proceedings FRAMCOS-3
AEDIFICATIO Publishers, D-79104 Freiburg, Germany

CRACK FORMATION AROUND AGGREGATES IN HIGH-SHRINKAGE CEMENT PASTE

B.F. Dela and H. Stang
Department of structural Engineering and Materials
Technical University of Denmark
Lyngby, Denmark

Abstract

An investigation of cracking around aggregates embedded in high-shrinkage cement paste has been carried out. For this purpose a set of models are set up to determine the stresses inside a cylindrical inhomogeneity as a result of shrinkage in the surrounding cement paste. The stress intensity factor at a crack tip near the cylinder is also included in the models. Results from calculations based on the models are compared with test results. The tests are carried out on specimens consisting of a granite cylinder embedded in a high shrinkage cement paste. The initiation of cracks and crack growth is studied as a function of time using a microscope.
Keywords: Eigenstresses, micro-cracking, cement paste, aggregate

1 Introduction

Shrinkage of cement paste restrained by the presence of aggregates will result in a clamping pressure on the aggregates and tensile stresses in the cement paste along the aggregate-paste interface. In some cases the combination of shrinkage and restraint (and flaw size) causes stresses of such magnitude that cracks will be initiated. The cracks will develop in radial direction perpendicular to the surface of the aggregate.

In concrete containing a high amount of microsilica apparent shrinkage cracking has been observed in thin sections. However, it is discussed whether cracks in thin sections developed already before preparing the sample, or if they were introduced by the preparations (saw-cut, drying, polishing etc.). To obtain reliable experimental data it is necessary to observe the development of a crack without the need for any mechanical preparations of the sample. The cracking process around an aggregate can be studied in a 2 dimensional cracking analysis using a cylindrical inhomogeneity as aggregate. The initiation of cracks can then be followed with the use of a microscope.

2 Analytical models

Two types of models are set up in the analysis. First, a linear elastic model will be used to estimate the eigenstresses caused by the autogenous shrinkage of the cement paste. The results from the linear elastic calculations will then be used in a fracture mechanical analysis.

2.1 Determination of eigenstresses

The pressure on a cylindrical inhomogeneity surrounded by a matrix undergoing a free shrinkage, ε_s, can be deduced from Timoshenko and Goodier (1970). The matrix is at this point assumed to be crack free. The system to be modeled is shown in Fig. 1.

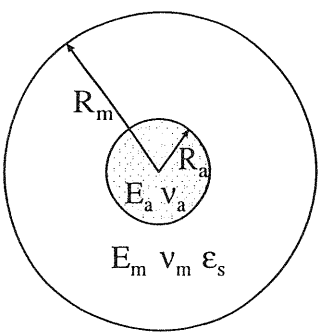

Fig. 1. Geometrical model considering a cylinder embedded in the center of a disc undergoing an overall shrinkage ε_s

A cylinder with radius R_a is embedded in a disc with radius R_m. The modulus of elasticity is given by E and Poisson's ratio is given by ν. Subscripts a and m represent cylinder (aggregate) and matrix respectively.

The resulting pressure, p, inside the cylinder is given by the following

Eqn. 1:

$$p = \frac{1-\nu_a(1+2k\nu_a)}{1-2\nu_a} \frac{E_a E_m \varepsilon_s}{E_a(1+\nu_m)+E_m(1-\nu_a(1+2k\nu_a))} \quad (1)$$

Here k is a constant equal to 1 in case of plane strain, and $k = 0$ in case of plane stress.

The material properties for the cement paste (E_m, ν_m, and ε_s) are developing with time. Therefore Eqn. 1 has to be calculated as an integral:

$$p(t) = \int_0^t \frac{(1-\nu_a(1+2k\nu_a))\, E_a E_m \dot{\varepsilon}_s}{(1-2\nu_a)\,(E_a(1+\nu_m)+E_m(1-\nu_a(1+2k\nu_a)))} dt \quad (2)$$

where $\dot{\varepsilon}_s$ is the rate of autogenous shrinkage.

2.2 Fracture mechanical analysis

Using the stresses as determined in the linear elastic model we can now perform a fracture mechanical analysis similar to the one proposed by Leung (1997). The analysis includes an upper and a lower limit by assuming two types of boundary conditions between matrix and cylinder. The lower limit for the critical stress intensity factor is deduced by assuming a perfectly smooth interface without any friction. The solution for this situation was obtained by Newman (1971). The upper limit is determined by considering perfect bond in the interface. This solution is derived by Leung (1997). The two situations are outlined in Fig. 2.

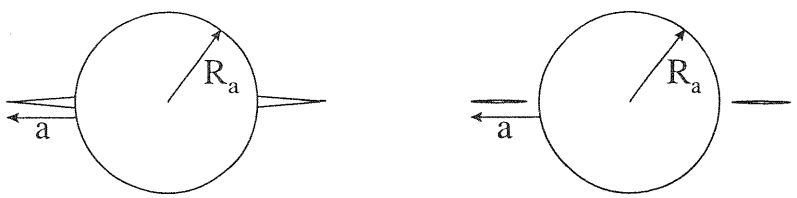

(a) Perfectly smooth interface

(b) Perfect bond in interface

Fig. 2. The two types of models used in the fracture analysis

The stress intensity factor for a perfectly smooth interface is given by

$$K = \frac{2p\sqrt{R_a}}{\sqrt{\pi(1+a/R_a)}} F_0 \quad (3)$$

The stress intensity factor for a perfect bond between the cylinder and the matrix is given by Leung (1997) as:

$$K = p\sqrt{R_a}\sqrt{\pi(a/R_a)}F_1 \tag{4}$$

The two factors F_0 and F_1 are functions of the crack length a normalized with the radius R_a of the cylinder. The two factors are shown graphically in Fig. 3.

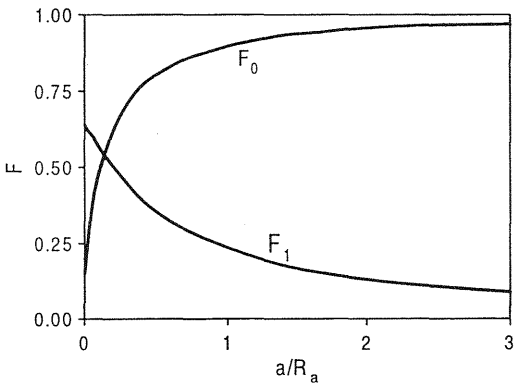

Fig. 3. The factors F_0 and F_1 as functions of normalized crack length a/R_a

The critical pressure p_{cr} can be determined by inserting the critical stress intensity factor K_{cr} in Equations 3 and 4. The critical stress intensity factor is defined as

$$K_{cr} = \sqrt{\frac{E_m G_F}{1 - k\nu_m^2}} \tag{5}$$

where k is the constant introduced earlier ($k = 0$ for plane stress and $k = 1$ for plane strain).

The critical pressure p_{cr} for a perfectly smooth interface becomes the lower limit p_{cr}^{low}:

$$p_{cr}^{low} = \frac{1}{2}\sqrt{\frac{E_m G_F \pi(1 + a/R_a)}{(1 - k\nu_m^2)R_a}}\frac{1}{F_0} \tag{6}$$

For a perfect bond in the interface we get the upper limit p_{cr}^{up}:

$$p_{cr}^{up} = \sqrt{\frac{E_m G_F}{(1 - k\nu_m^2)\pi R_a(a/R_a)}}\frac{1}{F_1} \tag{7}$$

In the present analysis the critical stress intensity factor is assumed to be independent of time. The critical pressure p_{cr} is calculated using a fixed modulus of elasticity of 22 GPa corresponding to cement paste older than 7 days.

3 Experiments and set-up

Experiments have been carried out in order to verify the models presented above. The mix considered in the experimental investigations contains white portland cement (wpc), microsilica (ms), superplasticizer (spc), and demineralised water (w). The composition of the mix was as follows: $\frac{w}{wpc} = 0.30$, $\frac{ms}{wpc} = 0.20$, $\frac{w}{wpc+ms} = 0.25$, and $\frac{spc}{wpc+ms} = 0.7\%$

The autogenous shrinkage is measured using a dilatometer (Jensen 1995). The measurements are carried out at a constant temperature of 20°C. The modulus of elasticity is determined by a curve-fit of test results from experiments carried out in uniaxial tension. The temperature of the specimens is kept constant at 20°C. The development of autogenous shrinkage and modulus of elasticity for the cement paste is shown in Fig. 4.

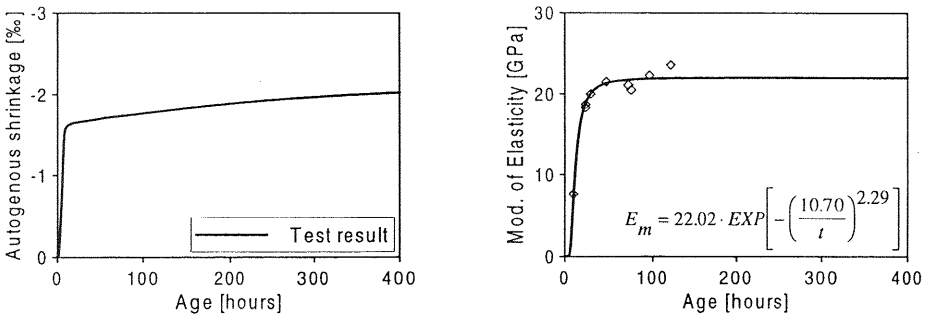

Fig. 4. Test results showing autogenous shrinkage and modulus of elasticity of cement paste as a function of time

The stiffness of the granite cylinder is determined in tests carried out in uniaxial compression. The modulus of elasticity is found to be 72 GPa. Poisson's ratio for the cement paste as well as for the granite is not determined experimentally. They are both assumed to be 0.2.

The fracture energy G_F of cement paste is determined using the method described in Dela and Stang (1997a). The G_F of the cement paste older than 7 days is 5 N/m for the cement paste used in the tests.

Furthermore, the cement paste is assumed to be linear elastic. Tests carried out on spherical inhomogeneities (Dela and Stang 1997b, Dela, Nielsen, Stang and Koenders 1997) have shown only weak visco-elastic behaviour in the 3 dimensional stress state present in the cement paste.

The set-up for the fracture experiments is made to suit the geometry in the models. A petri dish of glass was used as mould in the tests. A plate of teflon was placed in the bottom and the top of the mould in order to reduce the restraining effect from the mould when the cement paste shrinks. A granite cylinder with a radius of 10 mm and a height of 14 mm was placed

in the center of the mould. Two thin plastic strips were glued on opposite sides of the cylinder to create pre-cast notches. A series of 4 specimens were made for the testing. The two notches in the specimens had a length of 1 mm, 2.5 mm, 5 mm, and 10 mm respectively. The lengths of the notches were chosen with reference to Fig. 7 in order to get different critical stress levels. Cement paste was cast in a layer of 14 mm around the cylinder and vibrated. A teflon plate was placed on top before the mould was closed and sealed. After 1 day of hardening the mould was opened and the teflon plates were taken out. The specimens were replaced in the moulds and the moulds were sealed. During the short period each specimen was outside the mould, it was kept in a damp cloth to avoid drying of the specimen. The sealed moulds were kept in a climate chamber (temp=20°C, 40%RH) during the whole period of testing.

The specimens were studied under a microscope to follow the initiation of cracks at the notches. The observations were made without opening the glass moulds. The growth of the cracks were measured once each day (except weekends). In Fig. 5 a photograph of a 2.5 mm notch is shown. A small part of the granite cylinder can be seen on the left side of the photo.

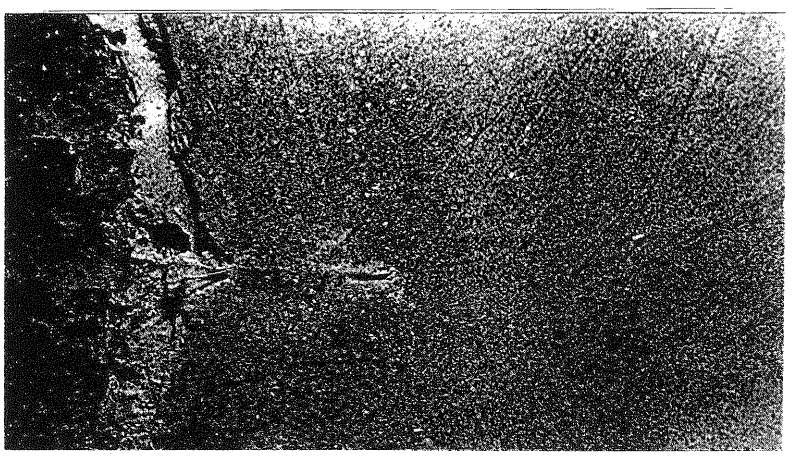

Fig. 5. Photograph of part of a test specimen showing a 2.5 mm notch before crack initiation

4 Results and discussion

Using the material properties as presented above the pressure on the cylinder is calculated according to Eqn. 2 using a time-increment of 15 minutes. The results are shown in Fig. 6.

The difference between the plane stress state and the plane strain state is small for the combination of materials used in the present investigation.

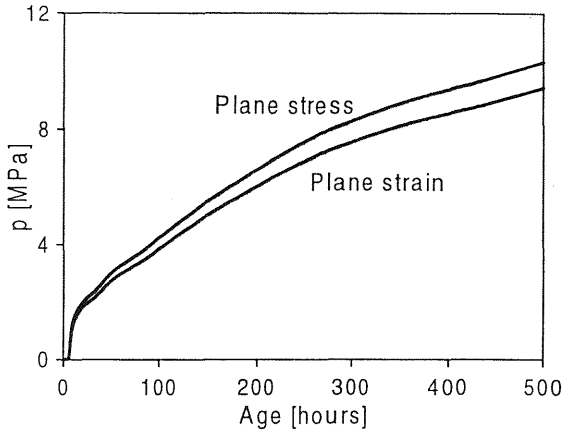

Fig. 6. The pressure inside and on the cylinder for plane stress and plane strain according to a linear elastic model

The difference will be larger for other combinations like steel and cement paste. However, the plane stress state will always show a larger pressure p than the plane strain state. This can be deduced from Eqn. 1.

Assuming a plane stress state on the surface and a plane strain state in the center of the specimen the cracks are expected to start at the surface. Since the cracks are observed on the surface, a comparison with the test observations should therefore be carried out for the plane stress state.

In Fig. 7 the critical pressure in a cylinder with a radius of 10 mm is shown for a perfectly smooth interface and for a perfect bond in the interface.

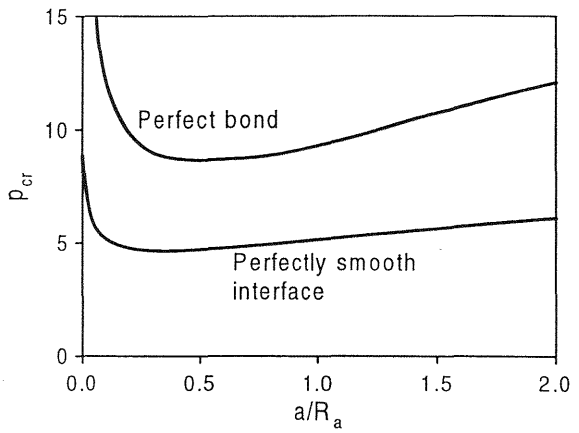

Fig. 7. The critical pressure in the cylinder as a function of normalized crack length a/R_a

The results shown in Fig. 7 show a clear dependency on the crack size. The most critical crack length (or flaw size) is between 0.2 and 0.7 times the radius of the cylinder.

Combining the results for plane stress in Fig. 6 with the critical pressure as shown in Fig. 7 it is possible to determine the critical age at which the pressure is equal to the critical pressure and a crack will propagate. In Fig. 8 the critical time as a function of normalized crack length is shown for perfect bonded interface and perfectly smooth interface, respectively. In the same figure experimental observations of crack length as a function of time after casting are shown. The dots represent the time at first crack observation at the notches. The experimentally measured crack length represents an average of the two notches in each specimen.

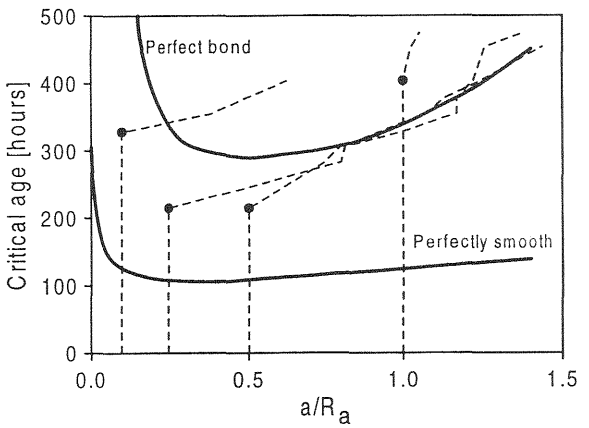

Fig. 8. The critical time (full lines) at which the crack will grow according to the models for perfect bond and for perfectly smooth interface respectively, shown together with experimental observations (broken lines) of crack length as a function of age of the specimens

The observations of crack initiation is in agreement with the calculations. Especially the time of crack initiation (shown with a bullet) for the 3 short notches (1 mm, 2.5 mm, and 5 mm) fall exactly in the middle of the predicted range. The first crack initiation of the longest notch of 10 mm is slightly later than the upper limit. As the bond in the interface is unknown it is not possible to estimate the effect of possible debonding in the interface between the cylinder and the cement paste. However, the cylinders used in the tests are cores and thus the surface is less rough than for instance the surface on crushed gravel. Thus some debonding could be expected near the notch.

For very short cracks (shorter than 0.2 times of the radius of the cylinder) the crack growth will start much later than for larger cracks. However, due to the smaller critical pressure for longer cracks (up to 1 times the radius),

the short crack will grow over a long distance when it is first initiated. This holds true only when disregarding the effect of stress release when the crack is opened. The stress release is probably the reason why a sudden crack growth was not observed in the specimen with the 0.1 mm notches.

It is important to emphasize that the calculated stresses are based on linear elastic models. This results in a higher calculated pressure than to be expected and thus the critical age is underestimated in the calculations.

Despite the numerous assumptions in the models, the results from the models are in very fine agreement with the test results.

Finally two pictures of a 2.5 mm notch are shown in Fig. 9. The upper picture shows the tip of the notch before a crack is initiated, whereas the lower picture shows the same notch tip after a crack is initiated.

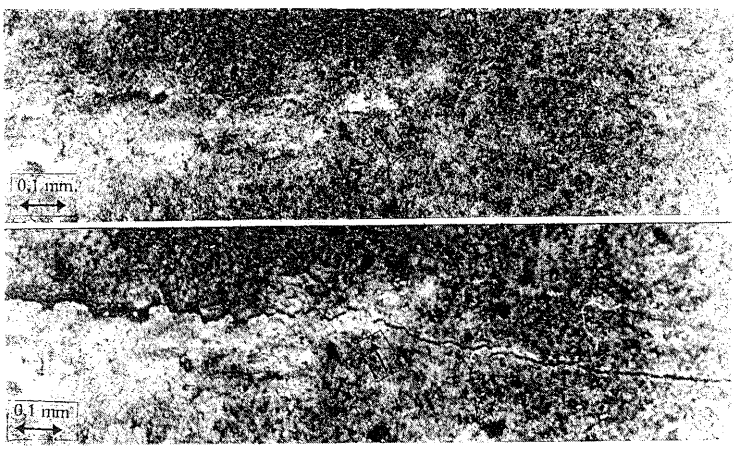

Fig. 9. Photographs of the tip of a 2.5 mm notch before and after crack initiation. The notch tips are indicated by arrows

5 Concluding remarks

The risk of matrix cracking around aggregates in high shrinkage concrete has been evaluated by simplifying the geometry into a 2 dimensional problem without neighboring aggregates. A granite cylinder embedded in a disc of neat cement paste is investigated experimentally. An estimation of the critical age when a crack of a certain length will propagate has been made by combining a linear elastic model with two fracture mechanical models. The linear elastic model determines the pressure inside and on the granite cylinder as a function of time by including the development of stiffness and shrinkage of the cement paste. The bond between the granite cylinder and the cement paste is unknown and hence two models were set up. One assuming full debonding on the interface and one assuming a perfect bond in

the interface. These two models provide an upper and lower limit for the critical pressure.

The models have been verified by comparing with results obtained through experiments. The experiments were carried out on disc-shaped specimens of cement paste. In the center of each specimen a granite cylinder was cast with two notches fixed to it. The specimens were examined under the microscope and the crack length as a function of time was observed. This includes the time of initiation of first crack.

The results from the models proved to be in perfect agreement with the test results. This indicates that it is possible to estimate the time of crack initiation in a 2 dimensional model when the sizes of flaws around the aggregates are known. The results showed that very small flaws and very large flaws are less critical than flaws in the range between 0.2 and 0.7 times the radius of the aggregate.

References

Dela, B. F., Nielsen, L. F., Stang, H. and Koenders, E. (1997). Eigenstresses in hardening concrete - a sensor for direct measurements, *in* A. Brandt, V. Li and I. Marshall (eds), **Brittle Matrix Composites 5 (BMC5)**, Woodhead Publishing Limited, Bigraf, 376–385.

Dela, B. F. and Stang, H. (1997a). Determination of fracture energy of cement paste cylinders in 3 point bending, *in* B. Karihaloo, Y.-W. Mai, M. Ripley and R. Ritchie (eds), **Advances in Fracture Research, ICF9**, Vol. 2, Pergammon, 927–936.

Dela, B. F. and Stang, H. (1997b). Internal eigenstresses in concrete due to autogenous shrinkage, *in* B. Persson (ed.), **Effect of Self-dessiccation in Concrete**, University of Lund.

Jensen, O. (1995). A dilatometer for measuring autogenous deformation in hardening portland cement paste, **Materials and Structures**, 28, 406–409.

Leung, C. K. (1997). Modelling of concrete cracking induced by steel corrosion, *in* A. Brandt, V. Li and I. Marshall (eds), **Brittle Matrix Composites 5 (BMC5)**, Woodhead Publishing Limited, Bigraf, 340–349.

Newman, Jr, J. (1971). An improved method of collocation for the stress analysis of cracked plates with various boundaries, **NASA**, TN D-6376, 1–45.

Timoshenko, S. and Goodier, J. (1970). **Theory of Elasticity**, third edn, McGraw-Hill.